2010

# Study of CFD Considering Valve Behavior in Reciprocating Compressor

Kenji Kinjo
*Appliances Development Center*

Akira Nakano
*Appliances Development Center*

Takumi Hikichi
*Appliances Development Center*

Koji Morinishi
*Dept. of Mechanical & System Engineering*

# Study of CFD Considering Valve Behavior in Reciprocating Compressor

Kenji KINJO[1]*, Akira NAKANO[1], Takumi HIKICHI[1], Koji MORINISHI[2]

[1]Appliances Development Center, Corporate Engineering Division,
Home Appliances Company, Panasonic Corporation
2-3-1-2 Noji-higashi, Kusatsu-shi, Shiga 525-8555, Japan
Phone: +81-50-3688-7417, Fax: +81-77-563-1967, E-mail: kinjo.kenji@jp.panasonic.com

[2]Dept. of Mechanical & System Engineering, Kyoto Institute of Technology
Matsugasaki, Sakyo-ku, Kyoto 606-8585, Japan

*Corresponding Author

## ABSTRACT

It is necessary to understand the behavior of the gas flows in the compression chamber generated by the driven piston, and the behavior of the reed valve that are opened and shut by the fluid force, when we reduce the loss of suction and discharge of the reciprocating compressor. To understand the above phenomenon, the moving object such as piston and reed valves is analyzed by applying virtual flux method and Cartesian grid that is suitable for expressing complex shape as main grid in this study.
In this paper, first, we introduce our numerical analysis method. Next, we introduce the verification by the comparison result between the above-mentioned analysis and the experiment.

## 1. INTRODUCTION

In recent years, efforts aimed at energy saving have been accelerating throughout the world from the perspective of conservation of the global environment. Including the Asian countries, where economic growth is marked, and the European countries, which are working positively on energy saving, energy saving regulations are becoming strict year by year. This trend has accelerated the energy saving competition among refrigerator manufacturers in domestic market and it will be necessary to develop higher efficiency reciprocating compressors in the future.
In such situation, the behavior of refrigerant in the compressor is analyzed by CFD (Computational Fluid Dynamics) to make concrete idea on the design, to minimize the test expenses and to accelerate the development when the reciprocating compressor is developed for the household refrigerator.
In the reciprocating compressor, the suction reed valve and the discharge reed valve are opened and shut by the fluid force of refrigerant compressed by piston in the compression chamber. Therefore, it is important for the improvement of performance of the reciprocating compressor to calculate the behavior of the refrigerant in the compressor with behavior of the reed valve accurately.
Recently, it begins to be used FSI (Fluid Structure Interaction) analysis that considers the behavior of suction reed valve and discharge reed valve. However, a general method of FSI analysis has some demerit that the mesh around the object is transformed and deteriorated.
Then, in this paper, it introduces following analysis method to solve the above problem. The three-dimensional compressible Navier-Stokes equations are used as the governing equations. The third-order weighted ENO (Essentially Non-Oscillatory) method is used for spatial discretization. The second-order Runge-Kutta method is used for time stepping. In addition, by applying virtual flux method to the moving objects, the flow driven by the piston of reciprocating compressor are obtained successfully on a single Cartesian grid.

## 2. CONSTRUCTION OF RECIPROCATING COMPRESSOR

The cross-section of a conventional reciprocating compressor is shown in Figure 1, and the basic construction of the suction and discharge paths is shown in Figure 2. The piston and cylinder mechanism is located in the upper side of the hermetic casing, while the motor is placed in the lower side. When the piston of this compressor moves toward bottom dead center (suction stroke), the pressure in the compression chamber reduces. Then the suction reed valve opens and refrigerant in the hermetic casing is guided into the compression chamber through the suction muffler, valve plate and suction reed valve. When the piston moves toward top dead center (compression stroke), the refrigerant in the compression chamber is compressed. Then the discharge reed valve opens and the refrigerant in the compression chamber flows out to the refrigeration system through the valve plate, discharge reed valve and cylinder head.

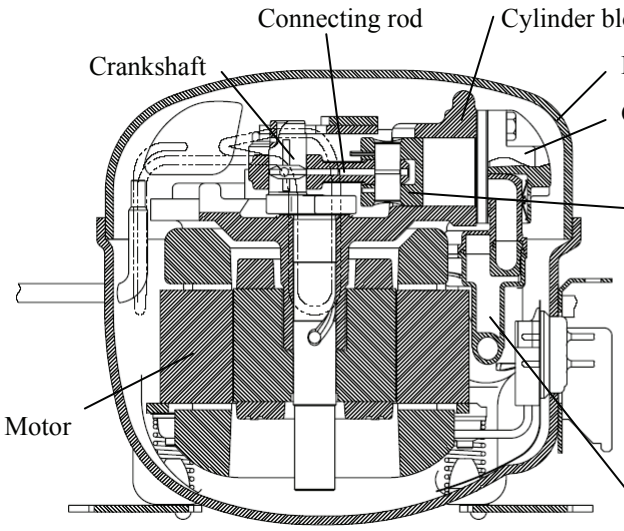


Figure 1: Schematic diagram of a reciprocating compressor

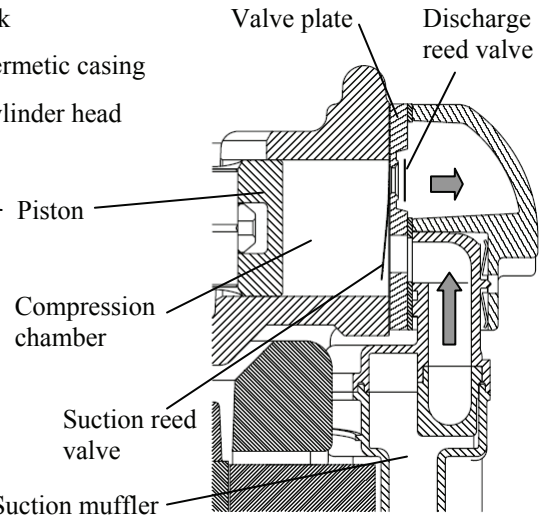


Figure 2: Close-up of suction and discharge paths

## 3. NUMERICAL PROCEDURE

Obtaining numerical solution of the compressible Navier-Stokes equations for flows about complex geometries on a Cartesian grid, the virtual flux method is introduced in conventional spatial discretizing methods.

### 3.1 Governing equations

Fluid flows in the reciprocating compressors may be described by the compressible Navier-Stokes equations, which can be written in the following form.

$$\frac{\partial \mathbf{q}}{\partial t} + \nabla \cdot \mathbf{F} = \nabla \cdot \mathbf{S} \tag{1}$$

The conservative vector and the flux vectors are given with:

$$\mathbf{q} = \begin{pmatrix} \rho \\ \mathbf{u} \\ e \end{pmatrix} \tag{2}$$

$$\mathbf{F} = \begin{pmatrix} \rho\mathbf{u} \\ \rho\mathbf{u}^2 + p\mathbf{I} \\ \mathbf{u}(e+p) \end{pmatrix} \tag{3}$$

$$\mathbf{S} = \begin{pmatrix} 0 \\ \tau \\ \mathbf{u}\cdot\tau - \mathbf{h} \end{pmatrix} \tag{4}$$

The total energy $e$ is defined for a perfect gas as:

$$e = \frac{p}{\gamma - 1} + \frac{1}{2}\rho\mathbf{u}^2 \tag{5}$$

The components of the viscous stress tensor and the heat flux vector, for example, $\tau_{xx}$, $\tau_{xy}$, and $h_x$, may be written as:

$$\tau_{xx} = 2\mu\frac{\partial u}{\partial x} - \frac{2}{3}\mu\left(\frac{\partial u}{\partial x} + \frac{\partial v}{\partial y} + \frac{\partial w}{\partial z}\right) \tag{6}$$

$$\tau_{xy} = \mu\left(\frac{\partial u}{\partial y} + \frac{\partial v}{\partial x}\right) \tag{7}$$

$$h_x = -\kappa\frac{\partial T}{\partial x} \tag{8}$$

In this study, Smagorinsky's eddy viscosity model is used for practical turbulent flow simulations.

### 3.2 Spatial discretizing method

The convective terms of the compressible Navier-Stokes equations can be evaluated simply at a regular point on the Cartesian grid, for example, as:

$$\left(\frac{\partial \mathbf{F}_x}{\partial x}\right)_i = \frac{\mathbf{F}_x\left(\tilde{\mathbf{q}}^+_{i+1/2}, \tilde{\mathbf{q}}^-_{i+1/2}\right) - \mathbf{F}_x\left(\tilde{\mathbf{q}}^+_{i-1/2}, \tilde{\mathbf{q}}^-_{i-1/2}\right)}{\Delta x} \tag{9}$$

where $i$ is the cell index as shown in Figure 3. The numerical flux at the cell surface is obtained as:

$$\mathbf{F}_x\left(\tilde{\mathbf{q}}^+_{i+1/2}, \tilde{\mathbf{q}}^-_{i+1/2}\right) = \frac{1}{2}\left\{\mathbf{F}_x\left(\tilde{\mathbf{q}}^+_{i+1/2}\right) + \mathbf{F}_x\left(\tilde{\mathbf{q}}^-_{i+1/2}\right) - \left|\mathbf{A}_x\right|\left(\tilde{\mathbf{q}}^+_{i+1/2} - \tilde{\mathbf{q}}^-_{i+1/2}\right)\right\} \tag{10}$$

where $\left|\mathbf{A}_x\right|$ is defined as:

$$\left|\mathbf{A}_x\right| = \mathbf{R}_x\left|\mathbf{\Lambda}_x\right|\mathbf{R}_x^{-1} \tag{11}$$

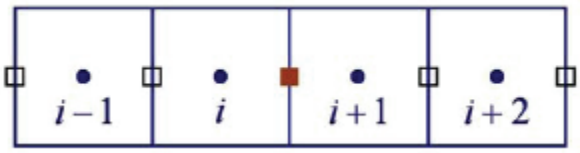


Figure 3: Stencil about a regular point

Here $\mathbf{\Lambda}_x$ and $\mathbf{R}_x$ are, respectively, the eigenvalue matrix and the right eigenvector matrix of the flux Jacobian matrix $\mathbf{A}_x$, which is defined as:

$$\mathbf{A}_x = \frac{\partial \mathbf{F}_x}{\partial \tilde{\mathbf{q}}} \tag{12}$$

The third order method may be obtained, for example, if $\tilde{\mathbf{q}}^-_{i+1/2}$ are evaluated with the following reconstruction.

$$\tilde{\mathbf{q}}^-_{i+1/2} = \tilde{\mathbf{q}}_i + \frac{1}{2}\left(\omega_0 \Delta\tilde{\mathbf{q}}_{i+1/2} + \omega_1 \Delta\tilde{\mathbf{q}}_{i-1/2}\right) \tag{13}$$

Here $\Delta\tilde{\mathbf{q}}_{i+1/2}$ are obtained with:

$$\Delta\tilde{\mathbf{q}}_{i+1/2} = \tilde{\mathbf{q}}_{i+1} - \tilde{\mathbf{q}}_i \tag{14}$$

The weights $\omega_0$ and $\omega_1$ for the third order linear method are:

$$\omega_0 = \frac{2}{3}, \quad \omega_1 = \frac{1}{3} \tag{15}$$

The weights $\omega_0$ and $\omega_1$ are defined for a nonlinear method as:

$$\omega_0 = \frac{2\alpha_0}{2\alpha_0 + \alpha_1}, \quad \omega_1 = \frac{\alpha_1}{2\alpha_0 + \alpha_1} \tag{16}$$

where $\alpha_0$ and $\alpha_1$ are obtained as:

$$\alpha_0 = \frac{1}{\Delta\tilde{\mathbf{q}}_{i+1/2} + \varepsilon}, \quad \alpha_1 = \frac{1}{\Delta\tilde{\mathbf{q}}_{i-1/2} + \varepsilon} \tag{17}$$

Here $\varepsilon$ is a small number which prevents null division in smooth flow regions.
The viscous terms of the Navier-Stokes equations are evaluated simply with the second order central difference approximation. For example,

$$\left(\frac{\partial \mathbf{S}_x}{\partial x}\right)_i = \frac{\mathbf{S}_x\left(\tilde{\mathbf{q}}_i, \tilde{\mathbf{q}}_{i+1}\right) - \mathbf{S}_x\left(\tilde{\mathbf{q}}_{i-1}, \tilde{\mathbf{q}}_i\right)}{\Delta x} \tag{18}$$

### 3.3 Virtual flux method

If an immersed solid boundary is located between the points *i* and *i*+1 as shown in Figure 4, the numerical fluxes of Equation (9) must be modified so that no-slip and no-penetration velocity boundary conditions are satisfied on the solid boundary.

$$\left(\frac{\partial \mathbf{F}_x}{\partial x}\right)_i = \frac{\mathbf{F}_x\left(\tilde{\mathbf{q}}^{*+}_{i+1/2}, \tilde{\mathbf{q}}^{*-}_{i+1/2}\right) - \mathbf{F}_x\left(\tilde{\mathbf{q}}^{*+}_{i-1/2}, \tilde{\mathbf{q}}^{-}_{i-1/2}\right)}{\Delta x} \tag{19}$$

where $\tilde{\mathbf{q}}^{*+}_{i+1/2}$, $\tilde{\mathbf{q}}^{*-}_{i+1/2}$, and $\tilde{\mathbf{q}}^{*+}_{i-1/2}$ are reconstructed with considering the immersed solid boundary conditions. For example,

$$\tilde{\mathbf{q}}^{*-}_{i+1/2} = \tilde{\mathbf{q}}_i + \frac{1}{2}\left(\omega_0 \Delta\tilde{\mathbf{q}}^{*}_{i+1/2} + \omega_1 \Delta\tilde{\mathbf{q}}_{i-1/2}\right) \tag{20}$$

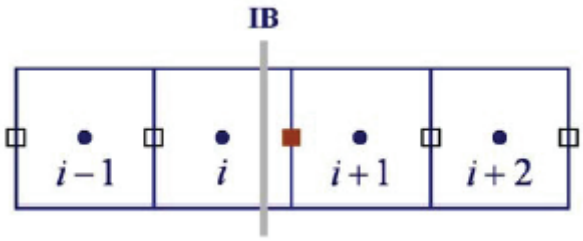


Figure 4: Stencil about a interfacial point

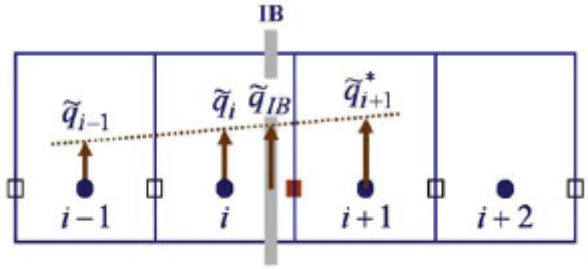


Figure 5: Stencil for one-sided extrapolation

where $\Delta\tilde{\mathbf{q}}^*_{i+1/2}$ calculated with:

$$\Delta\tilde{\mathbf{q}}^*_{i+1/2} = \tilde{\mathbf{q}}^*_{i+1} - \tilde{\mathbf{q}}_i \tag{21}$$

Here $\tilde{\mathbf{q}}^*_{i+1}$ are obtained with one-sided first or second order extrapolating operators $L$ as shown in Figure 5:

$$\tilde{\mathbf{q}}^*_{i+1} = L[\tilde{\mathbf{q}}_{i-1}, \tilde{\mathbf{q}}_i, \tilde{\mathbf{q}}_{IB}] \tag{22}$$

or

$$\tilde{\mathbf{q}}^*_{i+1} = L\left[\tilde{\mathbf{q}}_{i-1}, \tilde{\mathbf{q}}_i, \left(\frac{\partial\tilde{\mathbf{q}}}{\partial x}\right)_{IB}\right] \tag{23}$$

where $\tilde{\mathbf{q}}_{IB}$ and $\left(\frac{\partial\tilde{\mathbf{q}}}{\partial x}\right)_{IB}$ are Dirichlet and Neumann boundary conditions at the immersed boundary, respectively. The numerical viscous fluxes of Equation (18) must be also modified so that no-slip and no-penetration velocity boundary conditions are satisfied on the solid boundary as:

$$\left(\frac{\partial\mathbf{S}_x}{\partial x}\right)_i = \frac{\mathbf{S}_x\left(\tilde{\mathbf{q}}_i, \tilde{\mathbf{q}}^*_{i+1}\right) - \mathbf{S}_x\left(\tilde{\mathbf{q}}_{i-1}, \tilde{\mathbf{q}}_i\right)}{\Delta x} \tag{24}$$

### 3.4 Time stepping method

After discretizing the spatial derivatives, the Navier-Stokes equations can be written in the form:

$$\frac{\partial\mathbf{q}}{\partial t} = \mathbf{Q}(\mathbf{q}) \tag{25}$$

The second order Runge-Kutta method is used for solving the equation as:

$$\mathbf{q}^{n+1/2} = \mathbf{q}^n + \frac{1}{2}\Delta t\mathbf{Q}\left(\mathbf{q}^n\right) \tag{26}$$

$$\mathbf{q}^{n+1} = \mathbf{q}^n + \Delta t\mathbf{Q}\left(\mathbf{q}^{n+1/2}\right) \tag{27}$$

where the superscript $n$ denotes the time index and $\Delta t$ the time step size.

## 4. APPLICATION TO RECIPROCATING COMPRESSOR

In a reciprocating compressor, the suction and discharge reed valves are driven by the pressure force acting on them, while the piston is driven at a constant rate. Here the fluid-structure coupling simulation is carried out to reproduce the reed valve response and gas flows in the reciprocating compressor.

### 4.1 Reciprocating compressor model

The computational model of reciprocating compressor is drawn in Figure 6 schematically. The assumed motion of suction reed is described with the following equation of motion.

$$I\frac{d^2\theta}{dt^2} + k_s\theta = M \tag{28}$$

On the other hand, the assumed motion of discharge reed valve is described with the following equation of motion, because it thinks that it is opening and shutting a discharge reed valve to the discharge port as level approximately at the actual reciprocating compressor.

$$m\frac{d^2\lambda}{dt^2} + k_d\lambda = F \tag{29}$$

where spring stiffness of reed valve $k_s$ and $k_d$ gave a measured value.

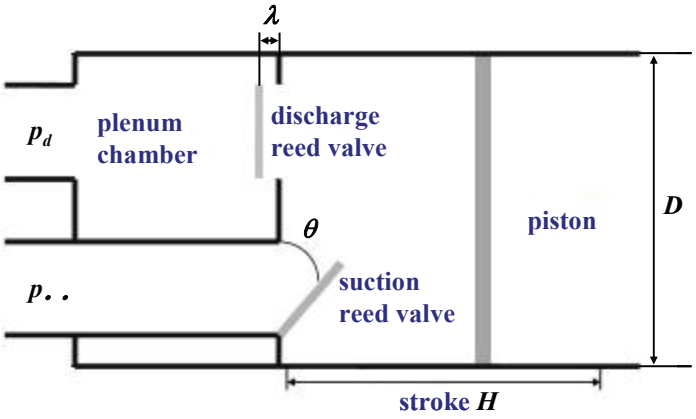


Figure 6: Shematic model of a reciprocating compressor

### 4.2 Comparison between the simulation result and the experimental result

The computation is carried out for the piston diameter $D$ of 20.6mm and stroke $H$ of 18mm. The piston is operated at the constant revolution rate of 3000 rpm. The pressure ratio of discharge pressure $p_d$ to suction pressure $p_\infty$ is 10. Typical velocity vectors, colored by the pressure obtained for suction and discharge strokes, are plotted in Figure 7 and 8, respectively. Fresh gases flow into the compression chamber through the suction port (Figure 7), and the gases are compressed and driven out through discharge port (Figure 8). The work of reciprocating compressor is clearly reproduced in the simulation.

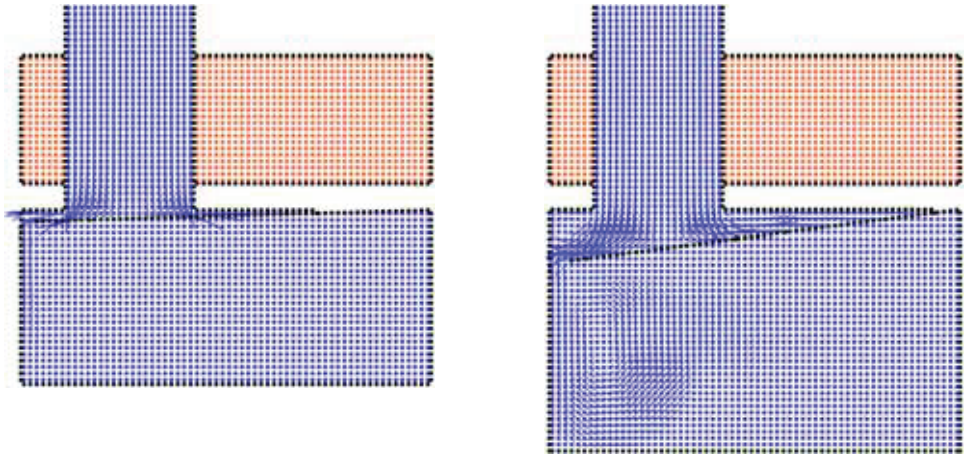

(a) (b)

Figure 7: Velocity vectors at an instant in suction stroke

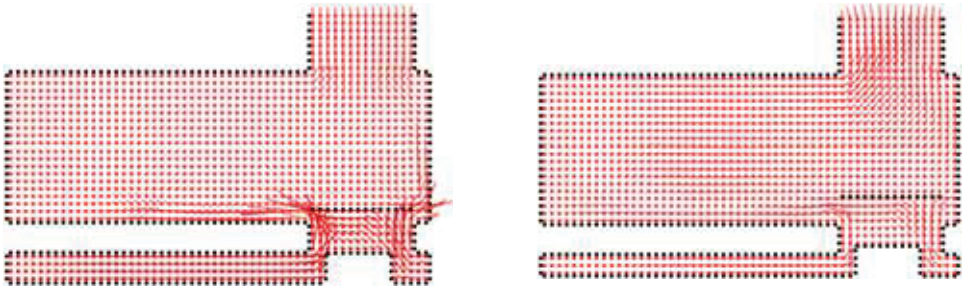

(a) (b)

Figure 8: Velocity vectors at an instant in discharge stroke

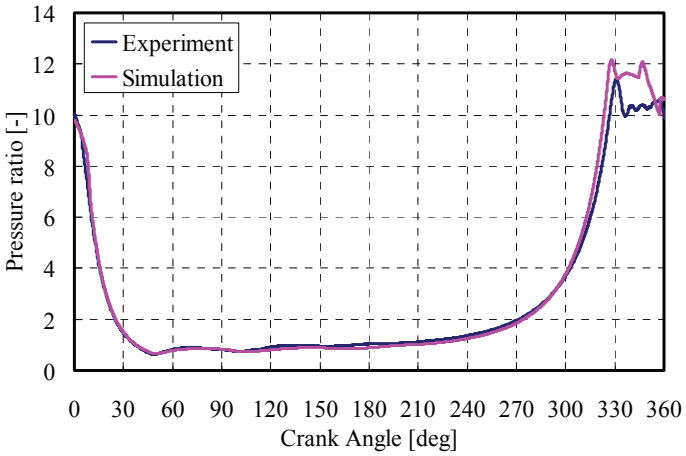


Figure 9: Comparison between simulation and experiment of pressure in compression chamber

Next, to verify the validity of the fluid-structure coupling simulation result, it evaluated in the comparison with the simulation result and the experimental result about the pressure variation in the compression chamber as shown in Figure 9.

Figure 9 shows that the pressure variation in compression chamber with suction and compression stroke agrees about the simulation result and the experimental result, being good comparatively. However, as for the simulation result, it shows that overpressure with discharge stroke is bigger than the experimental result, too. Probably, it thinks that the modeling of the discharge reed valve has a problem and that the above problem occurs with it and it is necessary to improve in the future.

## 5. CONCLUSIONS

The virtual flux method has been developed for simulating fluid-structure interaction problems. The numerical flux across the fluid-structure interface is successfully replaced with the virtual flux, so that proper interface conditions are satisfied there. In this study, the virtual flux method is applied to numerical flow simulations about reciprocating compressors. And it gives the fluttering reed valves of reciprocating compressor driven by the pressure force acting on them. After the first transition cycle, the compressor comes to work at almost constant flow rate. However, when comparing the simulation result and the experimental result, the accuracy for this simulation still has a problem. In the future, it solves the problem and then it utilizes for the development.

## NOMENCLATURE

| | | | |
|---|---|---|---|
| $e$ | Total energy per unit volume | $\mathbf{F}$ | Convective flux vector |
| $F$ | Force acting on reed valve | $\mathbf{h}$ | Heat flux vector |
| $I$ | Moment of inertia | $k$ | Spring stiffness |
| $M$ | Moment of force acting on reed valve | $m$ | Mass |
| $p$ | Pressure | $\mathbf{q}$ | Conservative vector |
| $\tilde{\mathbf{q}}$ | Primitive variable | $\mathbf{S}$ | Viscous flux vector |
| $\Delta t$ | Time step size | $T$ | Temperature |
| $\mathbf{u}$ | Velocity vector | $u$ | Velocity component |
| $v$ | Velocity component | $w$ | Velocity component |
| $\Delta x$ | Mesh spacing | $\gamma$ | Ratio of specific heats |
| $\theta$ | Open angle of reed valve | $\kappa$ | Thermal conductivity |
| $\lambda$ | Open distance of reed valve | $\mu$ | Viscosity |
| $\rho$ | Density | $\tau$ | Viscous stress tensor |

## REFERENCES

Jiang, G. S., Shu, C. W., 1996, Efficient Implementation of Weighted ENO Schemes, *Journal of Computational Physics*, vol. 126: p. 202-228.

Kim, J., Kim, D., Choi, H., 2001, An Immersed-Boundary Finite-Volume Method for Simulations of Flow in Complex Geometries, *Journal of Computational Physics*, vol. 171: p. 132-150.

Kim, J., Wang, S., Park, S., Ryu, K., La, J., 2006, Valve Dynamic Analysis of a Hermetic Reciprocating Compressor, *International Compressor Engineering Conference at Purdue*, C107.

Le, D. V., Khoo, B.C., Peraire, J., 2006, An immersed interface method for viscous incompressible flows involving rigid and flexible boundaries, *Journal of Computational Physics*, vol. 220: p. 109-138.

Nakano, A., Kinjo, K., 2008, CFD Applications for Development of Reciprocating Compressor, *International Compressor Engineering Conference at Purdue*, 1326.

Peskin, C. S., 1977, Numerical analysis of blood flow in the heart, *Journal of Computational Physics*, vol. 25: p. 220-243.

Tanno, I., Morinishi, K., Matsuno, K., Nishida, N., Validation of Virtual Flux Method for Forced Convection Flow, 2006, *JSME International Journal Series B*, vol. 49, no. 4: p. 1141-1148.

Udaykumar, H. S., Mittal, R., Rampunggoon, P., Khanna, A., 2001, A Sharp Interface Cartesian Grid Method for Simulating Flows with Complex Moving Boundaries, *Journal of Computational Physics*, vol. 174: p. 345-380.